Study on optimal impact damper using collision of vibrators

doi: 10.1016/j.jsv.2015.09.036

Title:

Study on Optimal Impact Damper Using Collision of Vibrators

Yoshio IWATA (Corresponding author)

Faculty of Mechanical Engineering, Kanazawa University

Kakuma-machi, Kanazawa 920-1192, Japan

e-mail iwata@se.kanazawa-u.ac.jp

Toshihiko KOMATSUZAKI

Faculty of Mechanical Engineering, Kanazawa University

Kakuma-machi, Kanazawa 920-1192, Japan

Satoshi KITAYAMA

Faculty of Mechanical Engineering, Kanazawa University

Kakuma-machi, Kanazawa 920-1192, Japan

Tatsuya TAKASAKI

West Japan Railway Company

289 Shinden-machi Hakusan 924-0015, Japan

Abstract

In this paper, we propose an impact damper which consists of multiple vibrators installed on a main structure and dissipates the vibrational energy by collisions between the vibrators. Transient vibration of the main system subject to an impact rapidly converges to zero by the impact damper. DE(Differential Evolution) method which is one of the optimization methods is employed to determine mass and spring constant of the every vibrators to maximize damping effect. We discuss the effect of a coefficient of restitution of vibrators, a ratio of total mass of the vibrators to the main structure mass and the number of the vibrators on the damping performance. The damping effect of the impact damper with three vibrators is demonstrated experimentally.

Key Words :Damping Effect, Optimal Impact Damper, Collision of Vibrators, Differential Evolution

1. Introduction

Methods for controlling the vibrations in structural systems can be categorized as passive or active. Passive methods control vibrations through the addition of dampers and dynamic dampers, which can be a single unit or a combination of elements such as springs, dampers, and masses. Active methods control vibrations through the installation of actuators. In terms of the installation and maintenance of control devices, passive methods are more cost-effective and are thus widely used today. In this report, we propose a passive vibration control method for structural systems subjected to impacts that uses an impact damper to dissipate the system's vibrational energy through collisions between vibrators.

Various vibration control devices for impacts have been proposed. For structural systems that experience harmonic external forces, dynamic dampers have been developed that control the structural vibrations through the addition of single-degree-of-freedom vibration systems such as spring, viscous damping, and mass [1]. Such dynamic dampers have been reported to also be effective in systems that receive impact forces [2]. However, it is not easy for dynamic dampers to realize the desired viscous damping. Practical applications of impact dampers include those with a single collision body enclosed in a container [3, 4] and granular dampers with many granules instead of collision bodies [5, 6]. Because of the nonlinear property on collisional vibrations, the damping effect is not proportional to the magnitude of the impact, and residual vibrations remain after the main collision ceases.

The proposed impact damper uses the collisions between multiple vibrators installed on the main structure with zero distance from each other. When the effect of the impact force is considered in terms of the initial velocity of the main structure, the response of the system with the vibrators is proportional to the initial velocity as described in Section 2. In this study, we used the optimization method of differential evolution (DE) and attempted to determine the masses and spring constants of the vibrators that maximize the damping effect. We carried out experiments to verify the damping effect of the proposed impact damper with three vibrators. We also investigated the effects of the coefficient of restitution, mass, and number of vibrators on the damping performance.

2. Principles and formularization of damper

Fig. 1 shows the model of the structure equipped with the proposed damper. The main structure consists of a single-degree-of-freedom structure with a mass m_0, damper c_0, and spring k_0. The main structure is equipped with n vibrators, each consisting of a collision body and cantilever beam. When the main structure experiences an external force $f(t)$ and starts vibrating, the vibrators start to collide with each other. The total energy of the system is dissipated through such repeated collisions to damp the vibration of the main structure. This is the damping principle of our device. We set the distance between the vibrators to zero so that they can collide even under small vibrations.

When masses of the collision bodies of n vibrators are represented with m_1, m_2, …, m_n, spring constants of the cantilever beams k_1, k_2, …, k_n, the displacements x_1, x_2, …, x_n, and the main structure's displacement x_0, the following equations hold for the motion of the model shown in Fig. 1.

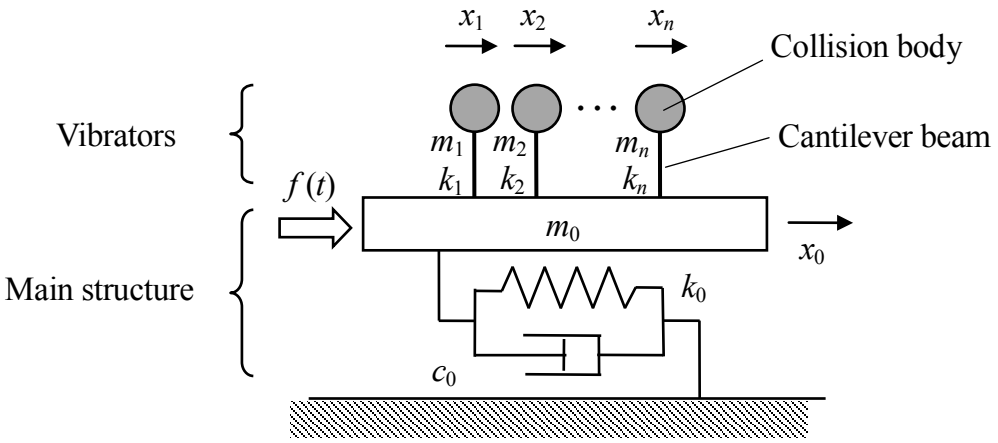

Fig. 1. Model of main structure and vibrators

$$\left.\begin{aligned} &m_0\ddot{x}_0 + c_0\dot{x}_0 + k_0x_0 - k_1(x_1 - x_0) - k_2(x_2 - x_0) - \cdots - k_n(x_n - x_0) = f(t) \\ &m_1\ddot{x}_1 + k_1(x_1 - x_0) = 0 \\ &m_2\ddot{x}_2 + k_2(x_2 - x_0) = 0 \\ &\quad\vdots \\ &m_n\ddot{x}_n + k_n(x_n - x_0) = 0 \end{aligned}\right\} \tag{1}$$

We considered the damping of the vibrators to be negligible. For simplicity, we considered the effect of the impact force $f(t)$ in terms of the initial velocity V_0 of the main structure mass m_0, i.e., $f(t) = 0$ in equation (1). We can then express this using matrices:

$$\boldsymbol{M}\ddot{\boldsymbol{x}} + \boldsymbol{C}\dot{\boldsymbol{x}} + \boldsymbol{K}\boldsymbol{x} = 0 \tag{2}$$

where

$$\boldsymbol{M} = \begin{bmatrix} m_0 & 0 & 0 & \cdots & 0 \\ 0 & m_1 & 0 & \cdots & 0 \\ 0 & 0 & m_2 & \cdots & 0 \\ \vdots & \vdots & \vdots & \ddots & \vdots \\ 0 & 0 & 0 & \cdots & m_n \end{bmatrix}, \quad \boldsymbol{C} = \begin{bmatrix} c_0 & 0 & 0 & \cdots & 0 \\ 0 & 0 & 0 & \cdots & 0 \\ 0 & 0 & 0 & \cdots & 0 \\ \vdots & \vdots & \vdots & \ddots & \vdots \\ 0 & 0 & 0 & \cdots & 0 \end{bmatrix},$$

$$\boldsymbol{K} = \begin{bmatrix} k_0 + k_1 + \cdots + k_n & -k_1 & -k_2 & \cdots & -k_n \\ -k_1 & k_1 & 0 & \cdots & 0 \\ -k_2 & 0 & k_2 & \cdots & 0 \\ \vdots & \vdots & \vdots & \ddots & \vdots \\ -k_n & 0 & 0 & \cdots & k_n \end{bmatrix}, \quad \boldsymbol{x} = \begin{bmatrix} x_0 \\ x_1 \\ x_2 \\ \vdots \\ x_n \end{bmatrix}$$

For the simulation, equation (2) was solved while the Newmark β method was used to consider the collisions between vibrators with zero initial displacements for the masses m_0, m_1, …, m_n , the initial velocity V_0 for m_0, and zero initial velocities for the masses m_1, …, m_n. Let the displacements of the vibrators at time $k\Delta t$ (i.e., the kth time period with the time interval Δt) be $x_1^{(k)}$, $x_2^{(k)}$, …, $x_n^{(k)}$. The condition for a collision between neighboring vibrators i and $i + 1$ with zero distance between them can be expressed as follows:

$$x_i^{(k)} \geq x_{i+1}^{(k)} \tag{3}$$

The following corrections are made so that the displacements, velocities, and accelerations of vibrators i and i+1 become those immediately after the collision. The displacements are corrected so that their intervals are all zero. Equation (4) presents the corrected displacements. Compared to the displacements $x_i^{(k)}$ and $x_{i+1}^{(k)}$, the corrected displacements are expressed as $x'^{(k)}_i$ and $x'^{(k)}_{i+1}$.

$$x_i'^{(k)} = x_{i+1}'^{(k)} = \frac{x_i^{(k)} + x_{i+1}^{(k)}}{2} \tag{4}$$

The velocities of the vibrators $\dot{x}_i^{(k)}$ and $\dot{x}_{i+1}^{(k)}$ calculated at $k\Delta t$ are those immediately before a collision. These velocities can be used to calculate the velocities $\dot{x}_i'^{(k)}$ and $\dot{x}_{i+1}'^{(k)}$ immediately after the collision. Using the law of conservation of momentum and the equations for the coefficients of restitution e of the vibrators, $\dot{x}_i'^{(k)}$ and $\dot{x}_{i+1}'^{(k)}$ can be derived as follows. Here, the coefficients of restitution of the vibrators were assumed to be the same.

$$\left.\begin{aligned} \dot{x}'^{(k)}_i &= \frac{(m_i - em_{i+1})\dot{x}_i^{(k)} + (1+e)m_{i+1}\dot{x}_{i+1}^{(k)}}{m_i + m_{i+1}} \\ \dot{x}_{i+1}'^{(k)} &= \frac{(m_{i+1} - em_i)\dot{x}_{i+1}^{(k)} + (1+e)m_i\dot{x}_i^{(k)}}{m_i + m_{i+1}} \end{aligned}\right\} \tag{5}$$

Using these displacements and velocities, the conditions after the time $(k + 1)\Delta t$ can be calculated through the sequential application of the Newmark β method. Repeatedly correcting the conditions in the same manner for each collision allows the responses of the main structure and vibrators to be obtained. The responses can be precisely calculated provided that Δt is small.

When equation (1) is solved with the Newmark β method, there are many coefficient parameters in the equations of motion, which makes investigating the change in the vibration response of the structure due to each parameter complex. To address this issue, we express equation (1), where $f(t) = 0$, with dimensionless parameters. This reduces the number of parameters to better capture the effect of each parameter on the damping effect. After equation (1) is divided by the initial velocity V_0 , it can be rearranged with the main structure's natural frequency $\Omega = \sqrt{k_0/m_0}$ and the non-dimensional time $\tau = \Omega t$ to obtain the following dimensionless equations of motion, where $(\cdot)'$ signifies a derivative with respect to τ .

$$\left.\begin{aligned}
&\ddot{\xi}_0 + 2\zeta\dot{\xi}_0 + \xi_0 - \mu_1\omega_1^2(\xi_1 - \xi_0) - \mu_2\omega_2^2(\xi_2 - \xi_0) - \cdots - \mu_n\omega_n^2(\xi_n - \xi_0) = 0 \\
&\ddot{\xi}_1 + \omega_1{}^2(\xi_1 - \xi_0) = 0 \\
&\ddot{\xi}_2 + \omega_2{}^2(\xi_2 - \xi_0) = 0 \\
&\quad\vdots \\
&\ddot{\xi}_n + \omega_n{}^2(\xi_n - \xi_0) = 0
\end{aligned}\right\} \tag{6}$$

Here, ξ_0 is the dimensionless displacement of the main structure, ξ_i (i = 1, 2, …, n) are the dimensionless displacements of the vibrators, ζ is the damping ratio of the main structure, μ_i (i = 1, 2, …, n) are the ratios of the vibrator masses m_i to that of the main structure m_0, and ω_i (i = 1, 2, …, n) are the ratios of the vibrators' natural frequencies to that of the main structure Ω. We summarize the dimensionless parameters as follows:

$$\tau = \Omega t\,,\quad \zeta = \frac{c_0}{2\sqrt{m_0 k_0}}\,,\quad \xi_0 = \frac{x_0}{V_0/\Omega}\,,\quad \xi_i = \frac{x_i}{V_0/\Omega}\,,\quad \mu_i = \frac{m_i}{m_0}\,,\quad \omega_i = \frac{\sqrt{k_i/m_i}}{\sqrt{k_0/m_0}} \qquad (i=1, 2, \cdots, n) \tag{7}$$

Because we non-dimensionalize the equation by the initial velocity V_0, we use 1 for the initial velocity when solving the non-dimensional equations of motion. That is, the non-dimensionalized equations are not affected by the initial velocity V_0. Therefore, equation (7) shows that the displacement of the main structure x_0 and vibrator displacements x_i are proportional to V_0. Therefore, the damping rate of the response wave amplitude does not depend on the magnitude of the impact force.

We can use the reduction rate of the total energy of the system to evaluate the damping effect of collisions between the vibrators. This quantity is defined as the ratio of the total mechanical energy of the system to that initially given by the external impact force. The initial mechanical energy of the system is given by the initial velocity of the main system, and that after the initial impact is the sum of the kinetic energy of the system and the potential energies of the springs. For non-dimensional equations of motion, the total energy reduction rate ε is as follows. Note that the non-dimensional initial velocity for m_0 is 1.

$$\varepsilon = \dot{\xi}_0{}^2 + \xi_0{}^2 + \mu_1\dot{\xi}_1{}^2 + \mu_1\omega_1{}^2(\xi_1 - \xi_0)^2 + \mu_2\dot{\xi}_2{}^2 + \mu_2\omega_2{}^2(\xi_2 - \xi_0)^2 + \cdots + \mu_n\dot{\xi}_n{}^2 + \mu_n\omega_n{}^2(\xi_n - \xi_0)^2 \tag{8}$$

Systems with shorter times required for the energy reduction rate to decrease to a certain value are considered to possess a large damping effect. For our study, we set this particular energy reduction level to 1%. As discussed above, the non-dimensional damping time required for the energy reduction rate to reach 1% does not depend on the magnitude of the impact force.

3. Optimization of vibrators for damping effects

3.1 Case with two vibrators

We simulated a case with two vibrators and changed the non-dimensional natural frequencies ω_1 and ω_2 in

small increments in order to derive the optimized conditions for the vibrators from the distribution of the non-dimensional time τ_1 required for the energy reduction rate to reach 1%. Although parameters such as the mass ratio μ_i and coefficient of restitution e affect the energy reduction rate, we set them to constant here and only considered the natural frequencies of the vibrators.

The two-dimensional color map in Fig. 2 shows the distribution of the damping time as the non-dimensional natural frequencies of the vibrators ω_1 and ω_2 were changed in the increments 0.01. The mass ratio, which was the same for all vibrators, the coefficient of restitution, and the main structure's damping ratio were $\mu = 0.013$, $e = 0.55$, and $\zeta = 0.002$, respectively. These values were chosen based on the experimental structures shown later. The combinations of ω_1 and ω_2 in dark gray required a shorter time for the energy reduction rate to reach 1%. Thus, they showed a larger damping effect. Fig. 2 represents the combination of ω_1 and ω_2 with the maximum damping effect using the white circle: $\omega_1 = 0.61$ and $\omega_2 = 1.29$. The damping time of this combination was 48.7. Because the area around the optimum point of ω_1 and ω_2 is in dark gray, the damping effect can be obtained without making fine adjustments to the natural frequencies of the vibrators. The gray scale distribution in Fig. 2 is also symmetric about the line $\omega_1 = \omega_2$. This indicates that the damping characteristics would be the same even if the natural frequencies of the two vibrators were switched. The damping times were longer around the line of $\omega_1 = \omega_2$. This is because the two vibrators were similar and thus moved in a similar manner, which made collisions between them infrequent.

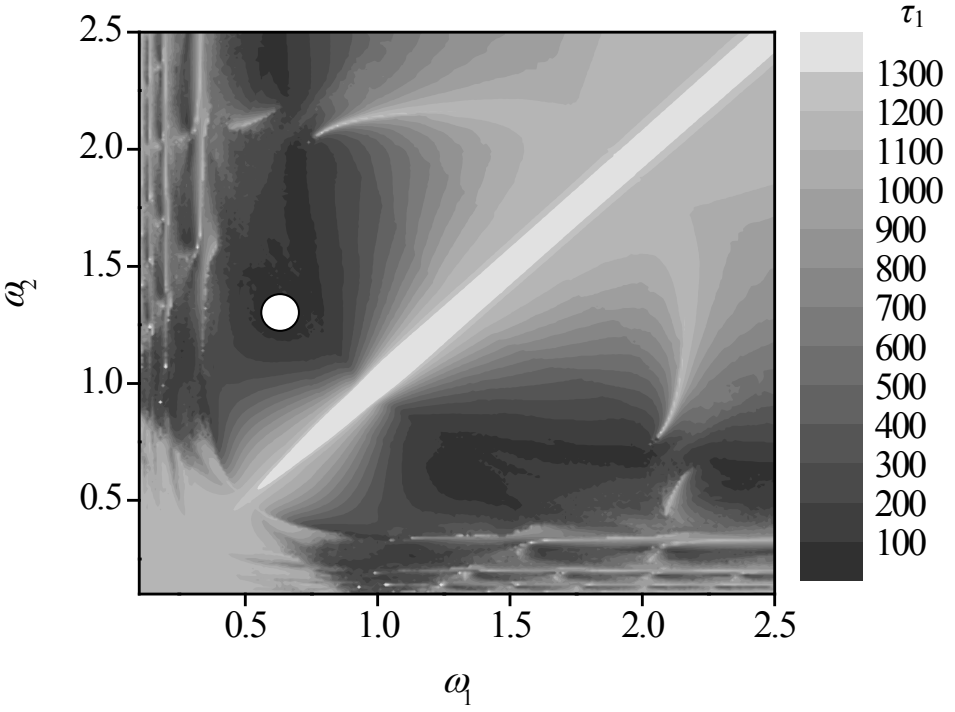

Fig. 2. Damping effect by vibrators with dimensionless natural frequencies ω_1 and ω_2
(μ=0.013, e=0.55, ζ=0.002)

Fig. 3(a) and (b) show the optimal response waveforms of the main structure and the vibrators respectively. The vertical axis indicates the non-dimensional displacement, and the horizontal axis is the non-dimensional elapsed time. The symbol ▼ indicates the time when the structure's total energy fell below 1 %. In Fig. 3(a), the

dotted line corresponds to the response without vibrators, and the solid line corresponds to the system with vibrators, which indicated faster damping. The waveforms of the vibrators in Fig. 3(b) show that periodic collisions between the two vibrators with opposing velocities (i.e., head-on collisions) seemed to increase the damping effect. Fig. 4 shows the change in the energy reduction rate with such collisions; there was a large decrease in the total energy with each collision. The response of the main structure increased after the time of the symbol ▼ in Fig. 3(a). On the other hand, the response of the vibrators decreased after the time of ▼ in Fig. 3(b), although the mechanical energy of the whole system changed slightly around the symbol ▼ as shown in Fig. 4. We consider that such responses were caused because the mechanical energy of the vibrators flowed into the main structure.

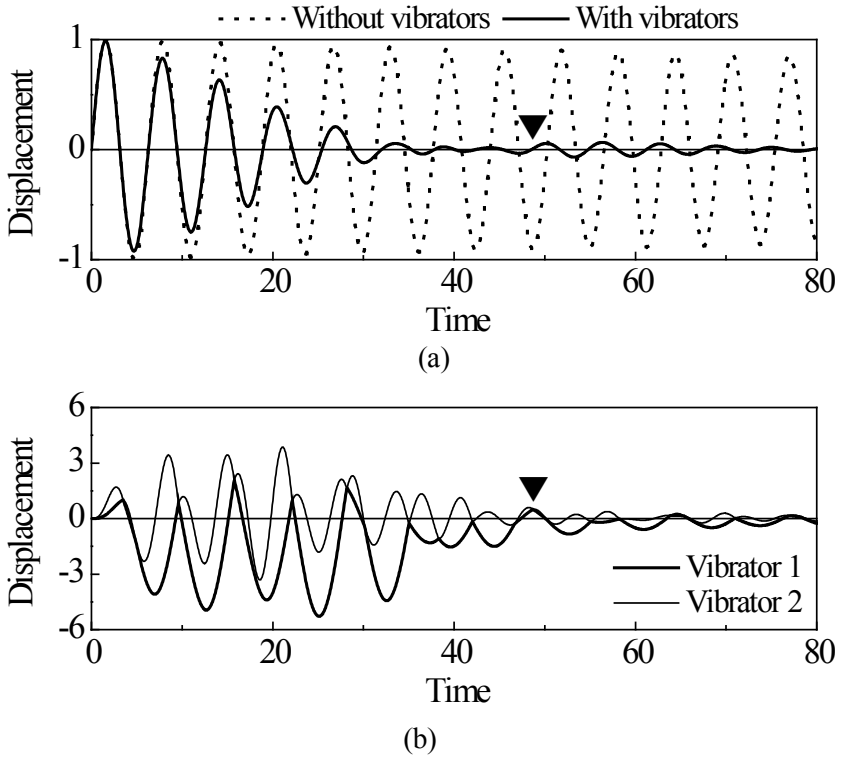

Fig. 3. Responses of system with two vibrators (μ=0.013, e=0.55, ζ=0.002). ▼: Time required for the energy reduction rate to reach 1%. (a)Main structure. (b)Two vibrators.

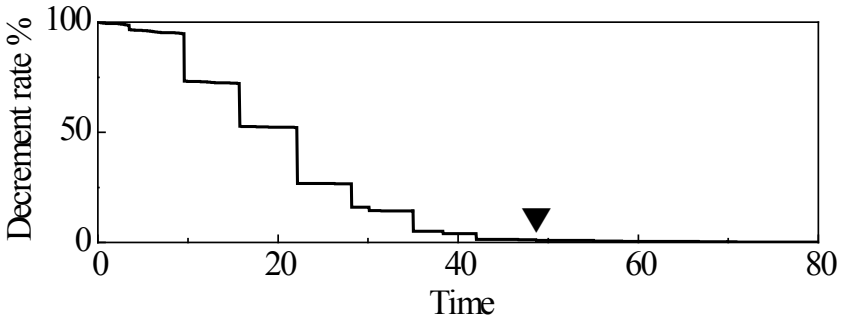

Fig. 4. Decrease of mechanical energy in two vibrators system (μ=0.013, e=0.55, ζ=0.002)

3.2 Optimization method: differential evolution

Increasing the number of vibrators should lead to a larger damping effect. However, an enormous amount of

time and labor would be needed to estimate the optimal combination of vibrators' natural frequencies by changing them in small increments. To solve this issue, we used the DE method [7], which searches for optimal values to more quickly identify the optimal vibrator conditions. DE is one of the population-based optimization methods. It allows for a simultaneous search of the entire domain of the design variables and can identify the minimum or maximum of the objective function for the entire range (global optimal solutions). First, an initial search group is randomly created, and the global optimal solution of the objective function is searched for through the repetition of operations such as mutation, intersection, and survival of the fittest. This method is similar to the concept of the genetic algorithm (GA), but the former treats solutions as numerical values themselves, so there is no need to create genes as in the latter. The detailed procedure of DE is described in Appendix.

DE is also said to have better convergence than the GA. DE does not require the gradient of the function, which makes it suitable for combination problems such as in our case. In order to verify DE's optimization, we searched for the optimal solution when $0.1 < \omega_1 < 2.5$ and $0.1 < \omega_2 < 2.5$, as given in Fig. 2. Because there are many local solutions, we ran several optimization calculations and attempted to identify the point with the shortest time for the energy reduction rate to reach 1%. We obtained an optimal solution that matched the results in Fig. 2; thus, the effectiveness of optimization by DE was verified. We used multiple personal computers to calculate the results in Fig. 2, which took a total of more than 100 h to calculate. In contrast, the time it took for one DE optimization process was about 4 min, which proves the efficiency of DE for optimization.

3.3 Optimization of vibrators by DE

We searched for the optimal combinations of the vibrators' natural frequencies for systems with two–five vibrators and considered the effect of the number of vibrators on the damping effect. For the vibrators, we kept the total mass ratios the same for all cases and used vibrators of the same mass in each case. We set the ratio of the total vibrator mass to the main structure mass to 0.06 and set μ to 0.03 for two vibrators, 0.02 for three vibrators, 0.015 for four vibrators, and 0.012 for five vibrators. The coefficient of restitution of the vibrators was $e = 0.55$ in all cases. We set the damping ratio of the main structure to $\zeta = 0.002$, as in the simulation described above. The search range of the natural frequency ω_i of each vibrator was set to 0.1–2.5, and we tried to identify the solution that minimized the time for the energy reduction rate to reach 1%.

Table 1 lists the optimization results for the cases with two–five vibrators. τ_1 is the non-dimensional time for the energy reduction rate to reach 1%, and ω_1–ω_5 are the natural frequencies of the vibrators that corresponded to the optimal condition. τ_1 decreased as the number of vibrators increased.

Table 1 Results of optimization in case of same mass ratio (Convergence condition 1%)

	μ	τ_1	ω_1	ω_2	ω_3	ω_4	ω_5
2 vibrators	0.030	37.1	0.593	1.32			
3 vibrators	0.020	27.6	1.45	0.817	0.671		
4 vibrators	0.015	24.7	1.54	0.405	0.360	1.24	
5 vibrators	0.012	22.1	1.80	1.16	0.100	1.05	0.742

Fig.5(a) and (b) show the responses of the main structure and vibrators, respectively, for the optimal case with two vibrators. At the non-dimensional time of 10, collisions between the vibrators occurred with a large relative velocity and thus led to a significant energy dissipation. After this point, the collisions repeated in synchronization with the vibration of the main structure, which effectively damped the vibration. The damping time was 37.1, while it was 48.6 in Fig. 2. This was mainly due to the increased vibrator mass ratio μ.

Fig. 6(a) and (b) show the responses of the main structure and vibrators, respectively, for the case with three vibrators. A collision between vibrators 1 and 2 was immediately followed by one between vibrators 2 and 3, and this process repeated in synchronization with the vibration of the main structure. Because of this, the time required for the energy reduction rate to fall below 1% was less than that in the case with two vibrators.

Fig. 7(a) and (b) show the responses of the main structure and the vibrators with four vibrators. In this case, collisions between the vibrators again occurred with the same frequency as the main structure vibration. As shown in Fig. 7(b), although it is difficult to discern because of the overlapping lines, vibrators 2 and 3 moved almost in unison at all times. Moreover, vibrators 2–4 moved in unison in one region, and vibrators 1–3 did so in the next region. This pattern was repeated in an alternating manner. As given in Table 1, ω_2 and ω_3 were lower than ω_1 and ω_4, which in turn indicates that the spring constants of vibrators 2 and 3 were smaller than those of vibrators 1 and 4. Therefore, vibrators 2 and 3 followed the movements of vibrator 1 or 4.

Fig. 8(a) and (b) show the responses of the main structure and the vibrators, respectively, in the case with five vibrators. In this case, the responses of vibrators 3–5 overlapped. Table 1 indicates that ω_3 and ω_5 were smaller than the others, which implies that vibrators 3 and 5 moved in unison with vibrator 4.

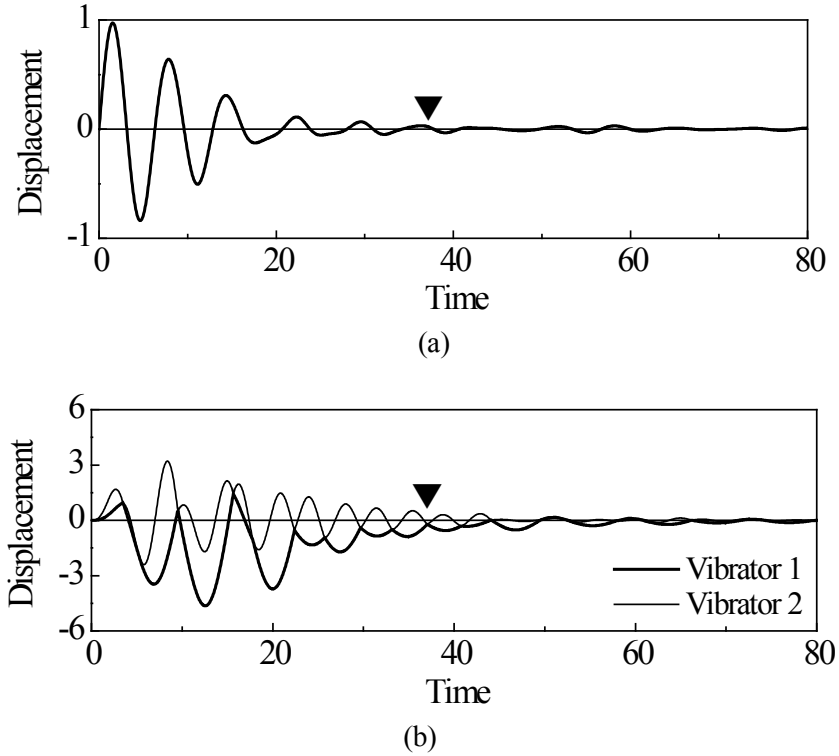

Fig. 5. Responses of system with two vibrators. (a)Main structure. (b)Two vibrators.

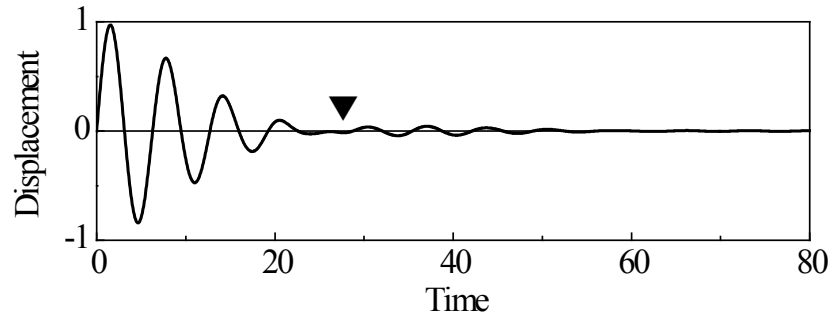

(a)

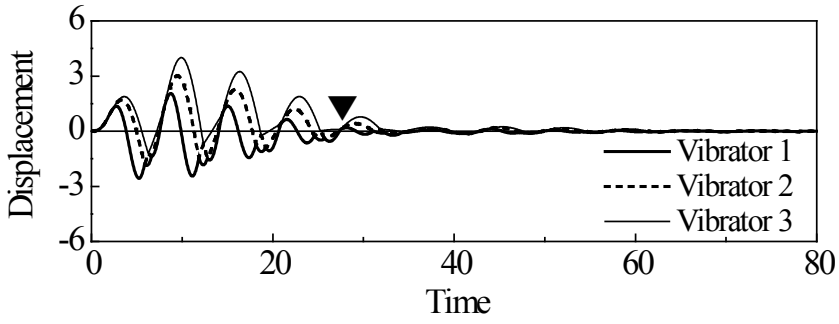

(b)

Fig. 6. Responses of system with three vibrators. (a)Main structure. (b)Three vibrators.

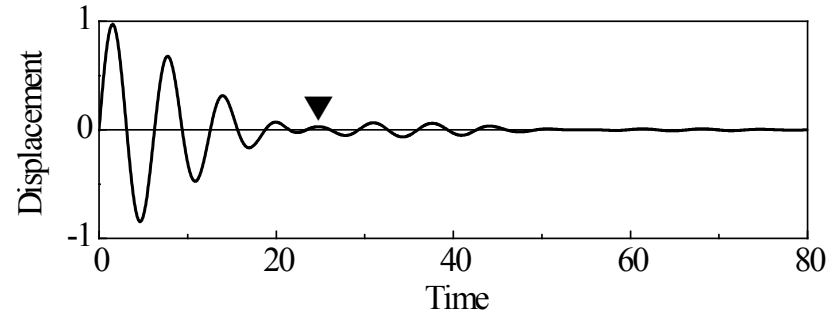

(a)

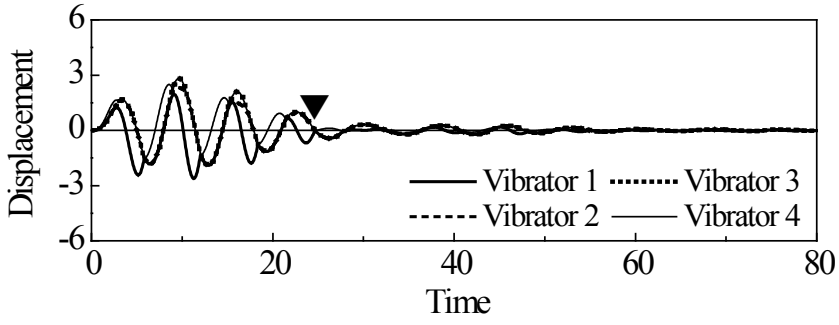

(b)

Fig. 7. Responses of system with four vibrators. (a)Main structure. (b)Four vibrators.

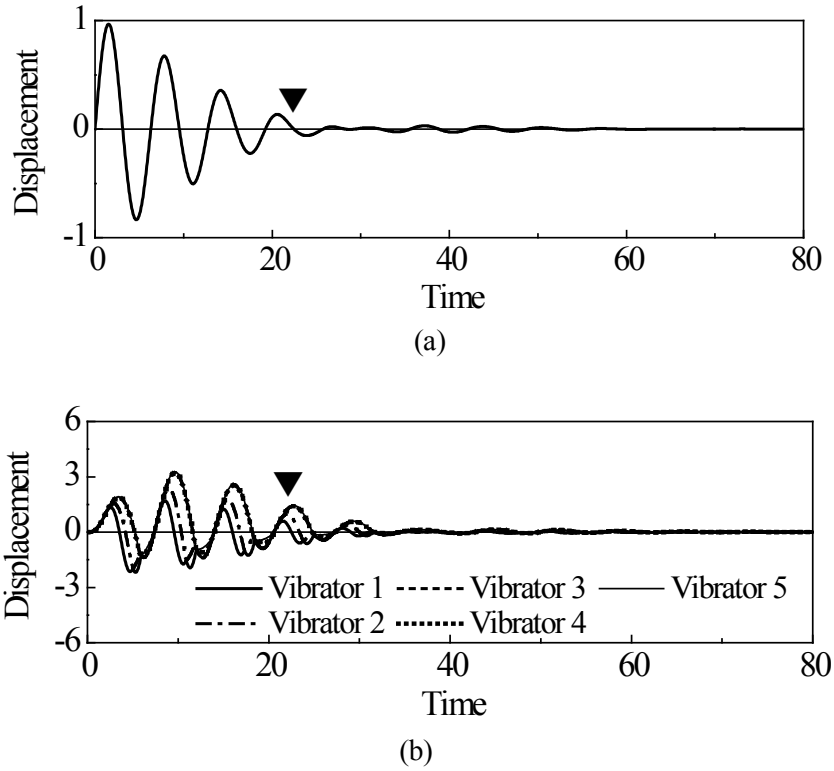

Fig. 8. Responses of system with five vibrators. (a)Main structure. (b)Five vibrators.

When the responses of the main structure with different numbers of vibrators are compared, the response waveforms overlapped until the third peaks, but the waveforms of the systems with more vibrators converged faster than those with less vibrators. This seems to be because a higher number of collisions leads to faster energy dissipation. Because the number of vibrators did not affect the damping effect until the third peak and the decrement of damping time required for the energy reduction rate to reach 1% becomes small, three vibrators are sufficient.

3.4 Effects of vibrator mass and coefficient of restitution

We previously set the mass ratio of the vibrators to the main structure to a constant 0.06. We then fixed the number of vibrators to three and investigated the effect of the mass ratio on the damping effect. We set the masses of the vibrators to be equivalent and varied the mass ratio μ per vibrator from 0.005 to 0.08 in increments of 0.001 to determine the non-dimensional time τ_1 for the energy reduction ratio to fall below 1%. Fig. 9 shows the results. Although τ_1 decreased as μ increased, it did not decrease smoothly. In particular, there were times when τ_1 made discrete changes. As shown in Fig. 4, this is because the energy reduction rate decreases discretely during moments of collision. When μ was higher than 0.04, τ_1 took at least three periods after an impact of the main structure to converge to a certain value. Thus, τ_1 tended to converge within the first three periods.

We then investigated the effect of the coefficients of restitution for the vibrators on τ_1. Fig. 10 shows τ_1 with a coefficient of restitution of 0.01–0.9 for the mass ratios per vibrator μ = 0.02 and 0.04. When the coefficient of restitution was 0.01–0.6, the changes in τ_1 were small for both mass ratios, and it could be considered constant. However, once the coefficient of restitution exceeded 0.7, τ_1 rapidly increased. With regard to the discrete

changes in τ_1, the same argument holds as in Fig. 9. When the cases with μ = 0.02 and 0.04 were compared, the larger μ corresponded to a smaller τ_1, but the change patterns of τ_1 were the same in both cases. Therefore, the effect of the coefficient of restitution on τ_1 is small and can be ignored as long as it stays below 0.6.

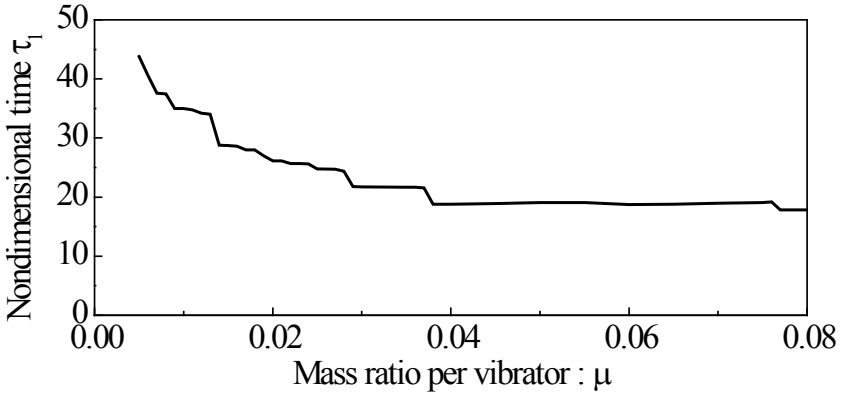

Fig. 9 Effect of mass ratio μ (With three vibrators)

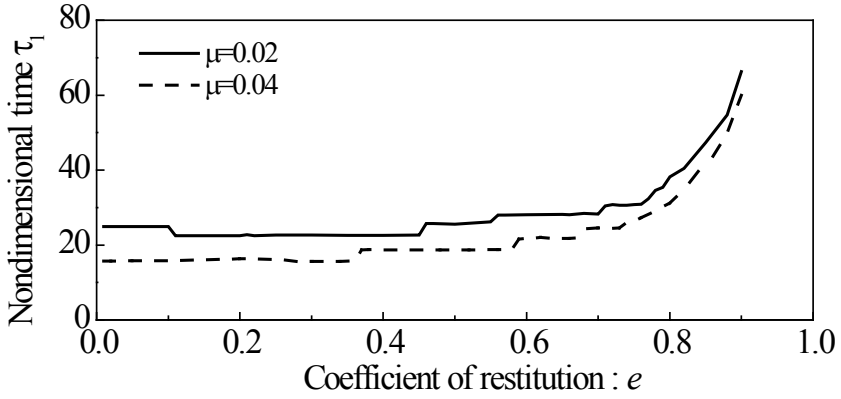

Fig.10 Effect of coefficient of restitution e (With three vibrators)

3.5 Comparison of a simple impact damper and an impact damper with two vibrators

The impact damper with two vibrators was compared with a simple impact damper described in the references [3] and [4]. Fig. 11 shows the simple impact damper system which consists of a main structure with mass m_0, damping coefficient c_0, spring constant k_0, and the impact damper with mass m and clearance d. The study in the reference [4] focused on the vibratory magnitude of the main structure after its initial displacement X_0, and showed that d=4cm presented the maximum damping effect when m_0=1kg, c_0=0, k_0=1N/m, m=0.05kg, e=0.5 and X_0=1cm. The maximum value of the waveform in this case approximately changed along the solid and the broken straight lines in Fig. 12, where the solid straight line showed the maximum value of the damped free vibration and the broken one the maximum value of the residual vibration (cf. Reference [3]). We equipped the main structure with two vibrators whose masses, m_1 and m_2, were 0.025kg, i.e., the total mass of the vibrators was equal to the simple impact damper mass. The coefficient of restitution between the vibrators was 0.5. Spring constants of the two vibrators were optimized under the condition that the main structure and all of the vibrators were displaced 1cm initially. The optimized spring constants k_1 and k_2 became 0.329 and 1.857, respectively. As shown by the solid curve in Fig. 12, the vibration of the main structure with two vibrators is slightly smaller than that of the

simple impact damper. While the residual vibration remains in the case of using the simple impact damper because of c_0=0, the free vibration of the system with two vibrators converges to zero. Because the free vibration rapidly converges with increasing number of vibrators, the suggested damper is more effective than the simple impact damper.

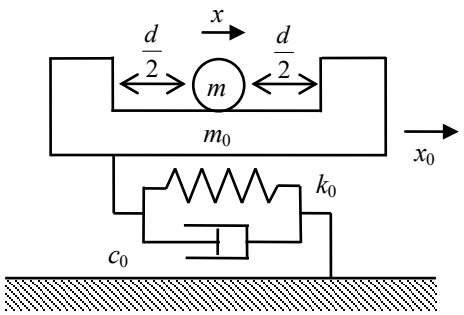

Fig.11 Simple impact damper system

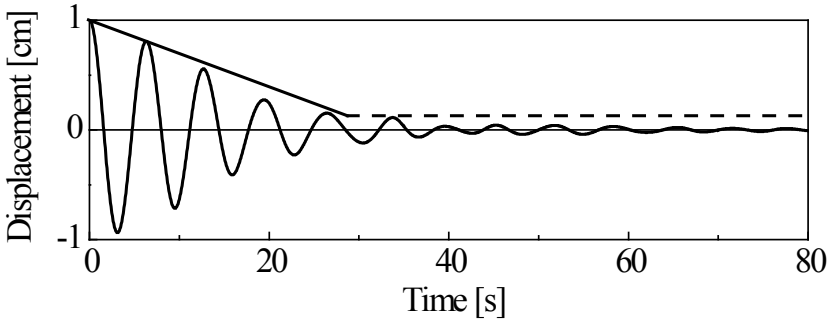

Fig.12 Comparison of main structure vibrations of simple impact damper and impact damper with two vibrators
Solid straight: Magnitude of damped vibration of simple impact damper
Broken straight: Magnitude of residual vibration of simple impact damper
Solid curve: Damped vibration of impact damper with two vibrators

4. Experimental investigation of damping characteristics

4.1 Experimental system and method

We created an experimental system with three vibrators and carried out damping experiments to determine the impact response of the system. Fig. 13 shows the experimental system. The main structure consisted of a duralumin board with a length of 300 mm, width of 180 mm, and thickness of 12 mm. The board was supported at a height of 170 mm by 0.8 mm thick phosphor bronze leaf springs at both ends. The duralumin board only vibrated to the right and left, as viewed in Fig. 13. The vibrators consisted of a collision body, a cantilever beam, and a coupler that connected the two. For the collision bodies, we used solid cylinders of silicone rubber with a diameter of 30 mm and length of 30 mm. The cantilever beams were made of phosphor bronze with a length of 74 mm from the fixed end and width of 10 mm, and the spring constant was adjusted through changes to the thickness. The coupler was made of duralumin material. We placed these vibrators on top of the main structure with zero distance from each other.

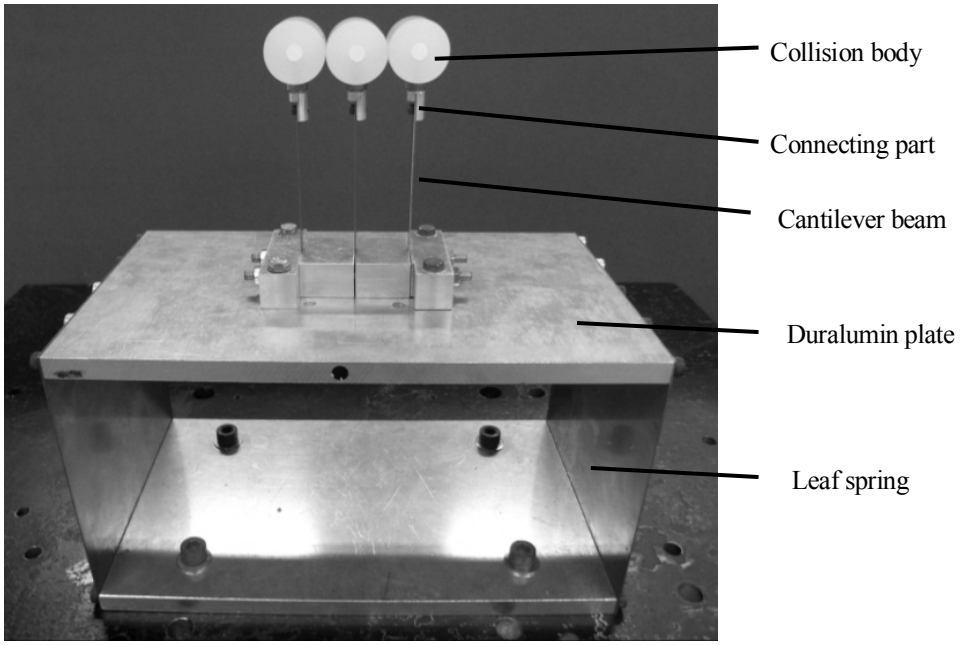

Fig.13 Picture of experimental system

Table 2 Experimental system parameters and optimal non-dimensional frequencies of vibrators

	Parameters of experimental system	Non-dimensional parameters of experimental system	Optimal non-dimensional frequencies
Main structure	m_0=2.26kg, k_0=6000N/m, c_0=0.47Ns/m	ζ=0.002	-
Vibrator1	m_1=0.030kg	μ_1=0.013	ω_{opt1}=0.56
Vibrator2	m_2=0.030kg	μ_2=0.013	ω_{opt2}=1.27
Vibrator3	m_3=0.030kg	μ_3=0.013	ω_{opt3}=0.95

Table 3 Practical parameters of vibrators

	Practical parameters	Practical non-dimensional frequencies
Vibrator1	m_1=0.030kg, k_1=25.0N/m	ω_1=0.56
Vibrator2	m_2=0.030kg, k_2=115N/m	ω_2=1.20
Vibrator3	m_3=0.030kg, k_3=73.4N/m	ω_3=0.96

The mass of the main structure m_0 consisted of the duralumin board, vibrator holder, and equivalent mass of the leaf spring to equal 2.26 kg, and the natural frequency of the main structure was measured to be 8.20 Hz. From this, the spring constant k_0 of the main structure was determined to be 6000 N/m. Based on the ratio of two successive amplitudes of the free vibration waveform with the main structure alone, the damping ratio ζ was determined to be 0.002. For each vibrator, the mass together with the collision bodies and coupler was 30 g, and we set m_1, m_2, and m_3 to this value. Thus, the mass ratios of each vibrator to the main structure μ_1, μ_2 and μ_3 were all 0.013. The coefficient of restitution between the collision bodies was measured to be 0.55. With the above non-dimensional parameters, we sought the optimal non-dimensional natural frequencies of the three vibrators with the shortest energy dissipation time. Table 2 presents the experimental system parameters and the optimal non-dimensional frequencies: ω_{opt1} = 0.56, ω_{opt2} = 1.27, and ω_{opt3} = 0.95. We then adjusted the thicknesses of the

cantilever beams so that the natural frequency of each vibrator would become close to the optimal values. The thicknesses were found to be 0.5 mm for vibrator 1, 0.8 mm for vibrator 2, and 0.7 mm for vibrator 3. Table 3 lists the measured values of the non-dimensional natural frequencies ω_1, ω_2, and ω_3 of the vibrators and the spring constants of each vibrator k_1, k_2, and k_3 as calculated from the vibrator masses. Although the natural frequencies of the vibrators were slightly different from the optimal values, a sufficient damping effect was obtained as long as these frequencies were close to the optimal values.

To determine the response of the main structure to an impact, we compared cases with and without the vibrators, and we confirmed the damping effect of the vibrators. For the impact given to the main structure, we dropped a mass suspended on a pendulum from a certain height to collide with the duralumin board and create an impact of a certain magnitude. We confirmed that the velocity V0 of the main structure immediately after the collision was 0.21 m/s. We used this value for the simulation and compared the results with those of the experiment. We took pictures of the main structure and vibrators for 3 s after the collision on a high speed digital camera at a speed of 1000 fps. We followed marks on the main structure and vibrators with image analysis software to measure the responding displacements.

4.2 Experimental results

Fig. 14 compares the response waveforms of the main structure with and without the three vibrators, as given in Table 3. The main structure's vibration decayed faster with the vibrators than without; thus, the results confirmed the damping effect of the impact damper with the vibrators.

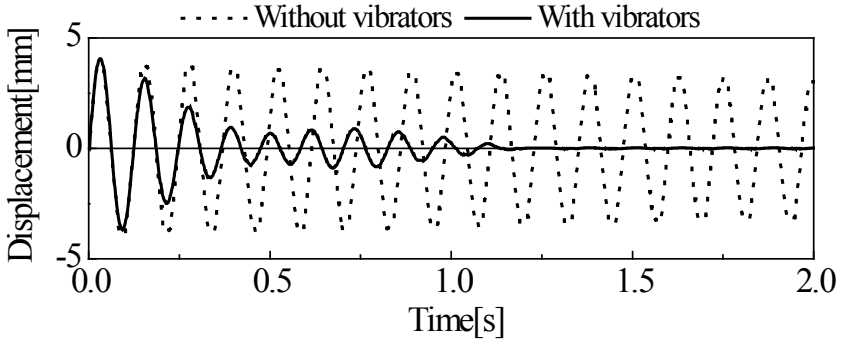

Fig.14 Main structure response in experiment

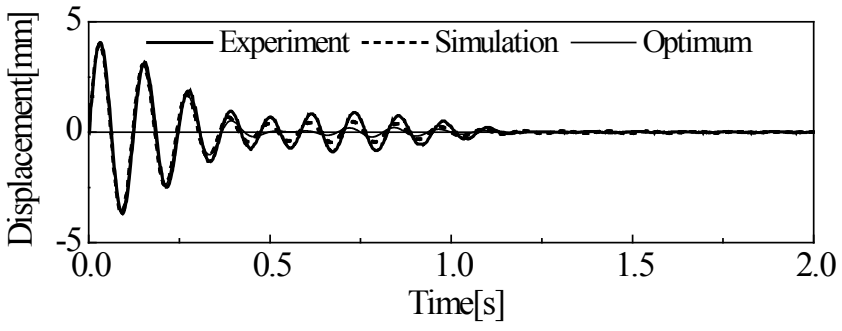

Fig.15 Comparison of experiment, simulation and optimal condition on main structure

Fig. 15 compares the corresponding displacements in the experiment and simulation. Fig. 15 also shows the response with the optimal condition given in Table 2. The three response waveforms in Fig. 15 are almost identical during the first two periods. After that, however, the amplitude was larger in the experiment, and the optimal condition had the smallest amplitude. The cylindrical collision bodies were placed at small relative angles, which led to an incomplete condition of zero intervals. The effect of this imperfection became conspicuous when the vibrators' vibrations became small, which presumably led the waveform to be larger than the other two waveforms. When the waveforms of the experiment and optimal condition were compared, the former was only slightly larger than the latter. This shows that vibrators with conditions close to the optimal condition can render similar damping effects to that of the optimal case.

Fig. 16(a) and (b) show the measured and simulated responses, respectively, of the vibrators. Similar to the main structure, the experimental response matched the one in the simulation in the initial periods. The increased difference after the initial periods was considered to be a result of the same reason given above. Also, Fig. 16(a) indicates that the rebound frequency of vibrator 1 was almost the same as that of the main structure. This implies synchronized collisions. The experimental results confirmed that such a phenomenon contributes to a larger damping effect.

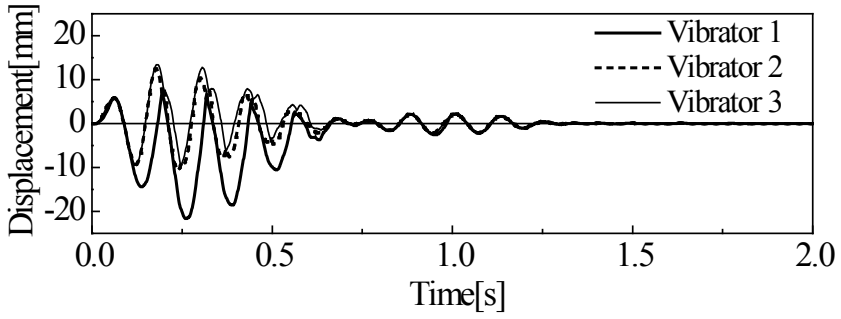

(a)

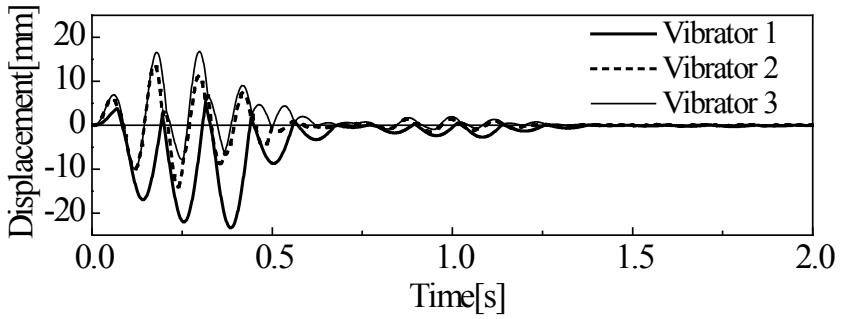

(b)

Fig. 16. Comparison between experiment and simulation on three vibrators. (a)Experiment. (b)Simulation.

5. Conclusion

We proposed an impact damper that uses the collisions of multiple vibrators to damp the vibrations of systems. We developed an optimization method for the vibrator parameters to maximize the damping effect and verified it experimentally. The results are summarized below:

(1) The vibrations of a main structure following an impact can be quickly damped by using the collisions between multiple vibrators. The amplitude of the vibration is proportional to the magnitude of the impact.

(2) DE can be used to optimize the vibrator parameters for the maximum damping effect.

(3) A system with three vibrators can damp the vibration of the main structure more quickly than one with two vibrators. However, a system with four or more vibrators shortens the damping time only slightly compared to a system with three vibrators.

(4) We carried out a damping experiment with three vibrators whose conditions were close to the optimal values and confirmed a damping effect similar to that obtained by a simulation.

(5) Based on the results of the numerical simulation and damping experiment, a large damping effect appears when vibrators collide consecutively in synchronization with the vibration of the main structure.

References

[1] J. P. Den Hartog, Mechanical Vibrations 4th Edition, McGraw-Hill, 1956.

[2] D. L. Bartel and A. I. Krauter, Time Domain Optimization of a Vibration Absorber, *Transactions of the American Society of Mechanical Engineers*, *Journal of Engineering for Industry* 93 (1971) 799-804.

[3] K. Yasuda and M. Toyoda., The damping effect of an impact damper, *Bulletin of the Japan Society of Mechanical Engineers* 21 (1978) 424-430.

[4] C. N. Bapat and S. Sankar, Single unit impact damper in free and forced vibration, *J Sound and Vibration* 99 (1985) 85-94.

[5] R. D. Friend and V. K. Kinra, Particle Impact Damping, *Journal of Sound and Vibration* 233 (2000) 93-118.

[6] M. Saeki, Impact damping with granular materials in a horizontally vibrating system, *Journal of Sound and Vibration* 251 (2002) 153-161.

[7] S. Kitayama, M. Arakawa and K. Yamazaki, Differential Evolution as the Global Optimization Technique and its Application to Structural Optimization, *Applied Soft Computing*, 11 (2011) 3792-3803.

Appendix: Differential Evolution

As described in section 3.2, the DE is one of the population-based optimization methods. Like other population-based optimization methods such as the genetic algorithm and the particle swarm optimization, several parameters (the number of search agents, the maximum search iteration number, the mutation ratio F, the crossover ratio Cr) should be set at first. In addition, there are various models in the DE, and the most basic model (DE/rand/1/bin) is used in this paper. The detailed procedure to find a global minimum by the DE is summarized as follows:

(STEP1) The number of search agents, the mutation ratio F, the crossover ratio Cr, and the maximum search iteration number $it_{\max}$ are set. The iteration counter it is initializes as it=1.

(STEP2) All search agents are generated at random in the design variable space.

(STEP3) The following procedure is applied to all search agents.

(STEP3-1) Agent d, denoted by $\boldsymbol{x}_d^{it}$, selects three search agents ($\boldsymbol{x}_{r1}^{it}$, $\boldsymbol{x}_{r2}^{it}$, $\boldsymbol{x}_{r3}^{it}$) at random, where $d \neq r1 \neq r2 \neq r3$

(STEP3-2: Mutation) New search agent denoted by $\boldsymbol{v}_d^{it}$ is generated by the mutation. The mutation in the DE is given by Eq.(A1).

$$\boldsymbol{v}_d^{it} = \boldsymbol{x}_{r1}^{it} + F(\boldsymbol{x}_{r2}^{it} - \boldsymbol{x}_{r3}^{it}) \tag{A1}$$

(STEP3-3: Crossover) Trial search agent denoted by $\boldsymbol{u}_d^{it}$ is generated by the crossover between $\boldsymbol{x}_d^{it}$ and $\boldsymbol{v}_d^{it}$.
(STEP3-4) Objective function is evaluated at $\boldsymbol{x}_d^{it}$ and $\boldsymbol{u}_d^{it}$, and then the search agent d is updated according to the following criteria.

$$\left.\begin{array}{l} f(\boldsymbol{u}_d^{it}) \le f(\boldsymbol{x}_d^{it}) \rightarrow \boldsymbol{x}_d^{it} := \boldsymbol{u}_d^{it} \\ f(\boldsymbol{u}_d^{it}) > f(\boldsymbol{x}_d^{it}) \rightarrow \boldsymbol{x}_d^{it} := \boldsymbol{x}_d^{it} \end{array}\right\} \tag{A2}$$

(STEP4) The iteration counter is increased $it := it + 1$.
(STEP5) If it is less than $it_{\max}$, return to STEP3. Otherwise, the algorithm will be terminated.

In the above flow, let us explain the crossover in STEP 3-3 for better understanding. $x_{d,i}^{it}$ represents the i-th design variable of $\boldsymbol{x}_d^{it}$, and $v_{d,i}^{it}$ also denotes the i-th design variable of $\boldsymbol{v}_d^{it}$. In the crossover, the crossover point is determined at random. The element of crossover point is inherited from $\boldsymbol{v}_d^{it}$, and the element of $\boldsymbol{u}_d^{it}$ that is a new point is determined. Secondly, random number r between 0 and 1 is generated to each design variable, and r is compared with the crossover ratio Cr. If r is less than Cr, the element of $\boldsymbol{u}_d^{it}$ inherits from $\boldsymbol{v}_d^{it}$. Otherwise, the element of $\boldsymbol{u}_d^{it}$ inherits from $\boldsymbol{x}_d^{it}$. Fig.17 is an illustrative example in the case of eight design variables.

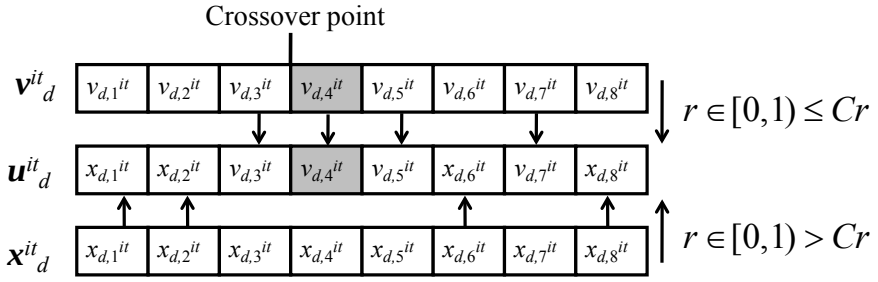

Fig.17 Crossover in DE

First, the crossover point is determined at random for determining the element of $\boldsymbol{u}_d^{it}$. In this example, the crossover point is 4-th design variable of $\boldsymbol{v}_d^{it}$. As the result, the element of $\boldsymbol{u}_d^{it}$ inherits from $\boldsymbol{v}_d^{it}$, as shown in Fig.17. Secondly, random number r is generated. If r is less than Cr, the element of $\boldsymbol{u}_d^{it}$ inherits from $\boldsymbol{v}_d^{it}$. Otherwise, the element of $\boldsymbol{u}_d^{it}$ inherits from $\boldsymbol{x}_d^{it}$. As the result, all elements of $\boldsymbol{u}_d^{it}$ are determined.